Influence of silver content on the tribomechanical behaviour on Ag-TiCN bioactive coatings

J.C. Sánchez-López[1], M.D. Abad[1], I. Carvalho[2], R. Escobar Galindo[3], N. Benito[4], S. Ribeiro[2], M. Henriques[5], A. Cavaleiro[6], S.Carvalho[2]

[1]Instituto de Ciencia de Materiales de Sevilla (CSIC-US), Avda. Americo Vespucio 49, 41092 Sevilla, Spain

[2]Universidade do Minho, Dept. Física, Campus de Azurém, 4800-058 Guimarães, Portugal

[3] Instituto de Ciencia de Materiales de Madrid (ICMM-CSIC), Cantoblanco, 28049, Madrid, Spain

[4] Departamento de Física Aplicada (CXII), Universidad Autónoma de Madrid, Cantoblanco, 28049, Madrid, Spain

[5] IBB-Institute for Biotechnology and Bioengineering Centre for Biological Engineering Universidade do Minho Campus de Gualtar, 4700-057, Portugal

[6] SEG-CEMUC Mechanical Engineering Department, University of Coimbra, 3030-788 Coimbra, Portugal

Abstract

Surface modification of bulk materials used in biomedical applications has become an important prerequisite for better biocompatibility. In particular, to overcome the particle generation, low-wear coatings based on carbon (nitrogen) and containing antimicrobial elements such as silver are promising candidates. Thus, the present work explores the potentialities of silver-containing carbonitride-based (Ag-TiCN) thin films prepared by direct current unbalanced reactive magnetron sputtering. The silver content in the coatings was varied from 0 to 26.7 at.% by changing the targets and the fraction of C_2H_2 and N_2 in the gas mixture with Ar. The obtained Ag-TiCN based coatings were characterized in terms of composition and microstructure. Mechanical and tribological properties of the films were studied by nanoindentation and reciprocating pin-on disk

testing in a fetal bovinum serum solution, respectively. Raman, SEM and energy dispersive X-ray (EDX) analysis was carried out in the contact region after tribological tests to obtain information about the friction mechanism. The cytotoxicity of the coatings was assessed by in vitro tests using fibroblast cells. The coatings comprised a mixture of TiC_xN_{1-x}, Ag and a-$C(N)_x$ phases whose relative proportion varied depending on the Ag/Ti ratio. The mechanical, tribological and cytotoxicity were correlated with the chemical and phase composition. When the Ag/Ti ratios were below 0.20 (Ag contents < 6.3 at.%) the films resulted harder (~18 GPa) with higher wear resistance (~10^{-6} mm^3/Nm), showing similar friction coefficient (~0.3) and good biocompatibility.

Keywords: Biocompatibility, silver, nanocomposite, amorphous carbon phases, tribology, fetal bovine serum, wear mechanism, cytotoxicity.

1. Introduction

Application of thin films in the biomedical engineering field represents an attractive challenge due to the multiple situations where they may improve or even functionalize a certain part of the human body. Although the use of hip implants is continuously increasing, implant failure is a huge problem for both the patient and governmental agencies, once it involves repeated surgeries and consequently considerable economical resources, as well as patients' death. This failure can be attributed to excessive wear and wear debris and also to microbial infection, which promotes the short durability [1]. For these reasons the investigation of new biomaterials is required to obtain good mechanical, tribological and biological properties that allow the development of better prosthesis. To overcome the problem of particle generation, the use of a very low wear coating material as diamond-like carbon (DLC), transition-metal carbides (MeC_x), nitrides (MeN_x), or others protective thin films, have been proposed [2-5].

In recent years, the research has been directed towards the use of antibacterial materials that could reduce the failure of medical devices provoked by the infections. Many of these studies focus on the use of silver, which is known to be an antimicrobial element [5-8]. When silver is transformed in ions and enters the environment, the multiplication of bacteria may be stopped because it is believed that Ag^+ absorbs the proteins of the cell wall [9]. The antibacterial activity is dependent on the total amount of Ag^+ ions which is responsible for the destruction of the bacteria. Conversely, if the quantity of silver released from the films is too high it can produce cytotoxicity [10]. Early works have studied the combination of hard phases (TiN or TiC), that provide hardness, with silver as soft metal to play the role of lubricant, to investigate their tribological performance [11,12]. For the use in artificial implants, good

biocompatibility is also required, in particular due to the known toxicity of the silver to the human body. In the last few years, the research efforts have been directed to assess the the biocompatibility of these multiphase nanocomposite materials with optimum tribological properties [5,6, 13-15]. We have investigated previously the deposition of TiC(O)N-based coatings by direct current (DC) magnetron sputtering gaining knowledge about the synthesis conditions that yielded a good compromise between tribological and hardness properties [16,17]. In the present study the addition of variable concentrations of Ag into TiCN films is explored with the goal of maintaining a good tribological performance without cytotoxicity effects. To achieve this purpose, the coatings are evaluated in terms of structure and composition and the tribological properties are studied in lubricated conditions using fetal bovinum serum (FBS) to simulate the biological conditions. The final mechanical and tribological performance is correlated with the evolution of the ratio of Ag/Ti inside the coatings as well as the effect of the Ag content in the cytotoxicity.

2. Experimental Details

Ag-TiCN samples were deposited by reactive DC magnetron sputtering using an Alcatel SCM650 apparatus onto polished and ultrasonically cleaned 316L steels and single crystalline silicon (100) substrates. Two types of targets (pure Ti and mixed Ti/Ag) of dimensions (200×100 mm^2) were used in $Ar+C_2H_2+N_2$ mixtures, with the substrates rotating at 70 mm over the target at a constant speed of 7 rpm. Argon flow was kept constant at 60 sccm while the reactive gases fluxes, C_2H_2 and N_2, were changed in the ranges of 5-11 and 5-12 sccm, respectively, in order not to change significantly the C and N contents. This represents a variation of the working pressure of the deposition chamber between 0.31 to 0.47 Pa. The films were grown at a constant

temperature (300 ºC) and bias voltage (-70 V). Varying the density of current applied to each magnetron and the chemical composition of the mixed Ti/Ag target, a set of samples was prepared with Ag content varying from 0 to 26.7 at. %. Further details about the synthesis conditions can be found elsewhere [18].

The atomic composition of the deposited samples was measured by electron probe microanalysis (EPMA) using a Cameca SX 50 apparatus. Ball crater tests were used to obtain the film thickness. The structure and phase distribution of the coatings were determined by X-ray diffraction (XRD) using a conventional Philips PW 1710 diffractometer, operating with Cu Kα radiation, in a Bragg–Brentano configuration. X-ray photoelectron spectroscopy (XPS) was measured using a hemispherical analyzer (SPECS EA-10 Plus) and Al K_α radiation as exciting source at a constant power of 300 W. The pass energy was 15 eV giving a constant resolution of 0.9 eV. The Ag 3d5/2 line at 367.9 was used to calibrate the binding energies. The samples were sputter-cleaned in situ using a broad 3 keV Ar^+ beam for 10 minutes.

Hardness measurements were conducted using a MicroMaterials Nanotest system equipped with a Berkovich indenter applying a maximum load of 10 mN. Correction of the geometrical defects in the tip of the indenter, thermal drift of the equipment and uncertainty of the initial contact was done [19]. The residual stresses, σ, were obtained by the deflection method from the Stoney's equation, using substrate curvature radii, both before and after coating deposition [20]. The tribological properties were evaluated by reciprocating friction tests using alumina-6-mm balls in diluted fetal bovine serum (FBS, 10% solution in water) in a CSM tribometer. The test parameters were set to 0.5 N of applied load; 3 mm/s of linear speed over a track length of 3 mm and 3000 cycles. The specific film wear rate was estimated after dividing the worn volume by the applied load and the sliding distance. Scanning electron microscopy (SEM) and energy

dispersive X-ray analysis (EDX) of the friction contact region were recorded in a FEG Hitachi S5200 microscopes operating at 5 keV. Raman spectra measurements (200-2000 cm^{-1}) were carried out in a LabRAM Horiba Jobin Yvon spectrometer equipped with a CCD (charge-coupled device) detector and a He-Ne laser (532 nm) at 5 mW.

Cytotoxicity tests were performed using fibroblasts 3T3 (CCL-163) obtained from American Type Cell Collection. Coated coupons (previously sterilized at 121ºC for 15 min) were inserted in six well plates and 3 ml of Dulbecco modified eagle medium DMEM (Gibco) were added to each well. The plates with the materials were then incubated with 5% CO_2 at 37ºC for 7 days. Meanwhile, the cells were grown in DMEM containing 10% of FBS (Gibco) and 1% penicillinstreptomicin, PS (Gibco). The cells were allowed to grow until attaining 80% confluence and after detachment 500 μL of cell suspension with $1x10^5$ cells/ml were added to each well of a 24 wells' plate. After 7 days of material contact with the medium, 500 μL were removed from each well and added to the plates with cells. The plates were incubated with 5% CO_2 at 37ºC for 48h. After that time, all the medium was removed and a solution containing 100 μL of MTS (3-(4,5-dimethylthiazol-2-yl)-5-(3-carboxymethoxyphenyl)-2-(4-sulfophenyl)-2H-tetrazolium, inner salt (Promega CellTiter 96® AQueous Non-Radioactive Cell Proliferation Assay) and 1 ml of DMEM without phenol red was added to each well. After 1 h, the absorbance of the resulting solution was read at 490 nm. The percentage of fibroblasts death was determined by the ratio of the difference between cell growth in the absence of Ag-TiCN sample (control – 100%) and the growth in the presence of a sample over the control growth. The assays were performed at least three times and in triplicate.

3. Results and discussion

3.1 Coating chemistry and microstructure

The chemical composition of the deposited coatings obtained by EPMA is shown in Table 1 together with the film thicknesses and the result obtained after evaluation of the tribo-mechanical properties. The carbon content do not vary significantly from 30 at.%. The N content decreases slightly from 33.9 to 21.8 at. %, the Ti content decreases from 36.9 to 17.9 at. % while the Ag content increases from 0 to 26.7 at %. Oxygen appears as contaminant in a range of 4-8 at.%, usually below 5 at.%. Since titanium and silver display an opposite trend, the Ag/Ti ratio will be used hereafter to label the samples and to discuss the changes observed in the structure and functional properties.

The XRD patterns obtained for the different Ag/Ti ratios are shown in Fig. 1. In the first sample (non-containing Ag) exhibit three reflections at 36º, 42º and 61º corresponding to the typical (111), (200) and (220) peaks originated by a cubic lattice whose positions lie intermediate between those for bulk TiC and TiN phases. By considering that the incorporated silver cannot form carbide or nitride phases and the complete mutual solid solubility of the TiN-TiC system, the formation of a TiC_yN_{1-y} phase is foreseen. A contribution to the peak shift due to the compressive residual stress in the coatings can be also possible. With the incorporation of silver, the TiC_yN_{1-y} diffraction peaks get broader and lose intensity concomitantly with the development of the characteristic pattern of metallic silver. In particular, for Ag/Ti ratios above 0.40 the main identified peaks correspond to fcc-Ag. The grain size of TiC_yN_{1-y} and Ag phases was determined by Scherrer formula using the (111) peak. The calculated values vary from 15 down to 9 nm and from 5 up to 8 nm, for TiC_yN_{1-y} and Ag respectively, with the increase of Ag/Ti. Under these premises, taking into account the atomic compositions given in Table 1, an excess of C and N is noticed over the Ti content and this difference becomes more significant as the Ag content increases. This can be

understood by assuming the formation of amorphous carbon-based phases (a-C and a-CN_x) where C atoms are connected to C or N atoms preferentially by sp^2 bonds, as observed in previous publications [21,22].

In order to obtain further information about these carbon-containing phases, XPS analysis was carried out on the C 1s and N 1s photoelectron spectra of Ag-TiCN coatings. Fig. 2a shows the C1s spectra for samples with Ag/Ti atomic ratios of 0, 0.20, 0.40 and 1.49. The spectra can be deconvoluted into four components at 282.0 (C-Ti), 283.2 (C-TiO), 285.1 (C-C) and 286.9 eV (C-N) bonds. The first conclusion that can be drawn from the analysis is the predominance of an amorphous carbon phase originated by the C_2H_2 precursor although a certain contribution from adventitious carbon cannot be discarded. The relative contribution of the carbide components (C-Ti and C-TiO) continuously decreases as the silver content increases, especially for the highest Ag/Ti ratios (0.40, 1.49), where the contribution of the C-C and C-N peaks is significantly higher. This results in agreement with the conclusions obtained previously attending to the changes denoted in chemical compositions and XRD data. In the N1s spectra of Fig. 2b, two contributions were found at 397.0 eV and 399.2 eV ascribed to N-Ti and N-C bonds, respectively. The intensity of the N-C component becomes significant when the Ag/Ti increases up to 0.40 and 1.49 (in agreement with the results for C1s spectra). By using the data obtained from the deconvolution of the N1s and the elemental chemical composition measured by EPMA it was possible to estimate the phase composition as a function of the Ag/Ti ratio. The obtained results are plotted in Fig. 3. The amorphous CN_x is slightly increasing while the main changes are noticed in the crystalline phases where the increment of Ag correlates with a diminution of the TiC_yN_{1-y} phase. This multiphase structure will certainly have an influence on the functional properties of the coatings (tribological, mechanical and biological) as we revise in the next sections.

Figure 4 shows the cross-sectional SEM micrographs of fractured Ag-TiCN samples with Ag/Ti ratios of 0, 0.20, 0.40 and 1.49. The film morphology displays a typical columnar-like microstructure although finer columns and porosity is observed as the Ag/Ti atomic ratio increases. This denser microstructure may be attributed to the segregation of the immiscible Ag and a-C(N) phases leading to renucleation sites that disrupts the columnar morphology. Similar behavior has been observed previously in Ag-CrN nanocomposites [23]. At the highest Ag/Ti ratio (Fig. 4d), Ag clusters are segregated to the column boundaries as observed before [14] which can be identified as brighter spots on the surface.

3.2. Mechanical properties: Hardness and residual stress

The hardness and internal stress values are presented in Fig. 5 as a function of the Ag/Ti ratio. The hardness varied in a range from 8 to 18 GPa, much lower than the typical values reported for pure TiCN coatings, ranging from 30 to 36 GPa [24-26]. These overall lower values should be certainly related with microstructural and chemical composition aspects. Thus, low energetic conditions of the deposition (low negative substrate bias and low deposition temperature) can lead to columnar and open morphologies. The phase composition of these nanocomposites is also affecting the dependence of the mechanical properties as it influences the balance between hard and soft phases and their distribution. Thus, according to the achieved accuracy increasing Ag content up to 6.3 at.% does not almost affect the hardness; however, further increase is accompanied with a significant hardness decrease. A similar behaviour of soft metals has been reported in the past in other systems, such as ZrN/Cu [27], ZrN/Ni [28], or others including silver, Ag/TiN [5] and Ag/TiC [29]. However, it is also likely that ion-induced defects in the films during the deposition or more compact film microstructure

would also contribute to this hardness enhancement. This would imply an increment of the compressive residual stress on the as-deposited coatings, as indeed was observed for Ag/Ti ratios lower than 0.2 (cf. Fig 5). Moreover, the decrease in the grain size, as a result of the interference of Ag deposition in the grain growth, promoting an increasing nucleation, can also contribute for the higher values of hardness.

Further increasing of the Ag/Ti ratio leads to a noticeable hardness reduction, in spite of the maximum in the compressive residual stress, mainly attributed to the increasing presence of either a boundary amorphous carbon-based phases (a-C and CN_x) or silver nanoparticles that softens the film structure as it was stated in previous studies [22,30]. By using the deconvolution of phases plotted in Fig. 3, the ratio of the soft phases ($Ag+CN_x$) vs. hard carbonitrides (TiC_yN_{1-y}) is calculated for establishing correlations with the tribo-mechanical properties. Thus, Fig. 6 clearly illustrates the dependence of the hardness versus this parameter. The wear rate is inversely proportional to the film hardness showing improved behavior at low $(Ag+CN_x)/TiC_yN_{1-y}$ ratios. Similar dependences have been reported in previous nanocomposites based on CrN/Ag; ZrN/Ag; TiN/Ag and TiN/Cu phases [14]. The excess of C and N segregates to surfaces and interfaces during film growth forming (C,N) – rich disordered region situated in the vicinity of TiC_yN_{1-y} grains causing an effective softening of the film. Moreover, the continuous increase on the Ag/Ti atomic ratio induces the nucleation of silver, a soft metal, which also contributes to further diminution of the hardness. The increment of the amorphous boundary regions led concomitantly to a decrease of the residual stress values as noted in Fig. 5.

3.3. Tribological properties: friction coefficient and wear rate

The tribological properties (friction coefficient and wear rate) were studied in lubricated conditions using 10% FBS solution in order to simulate the tribochemical conditions appearing in an artificial implant. Both properties are shown in Fig. 7a and 7b respectively, as a function of the Ag/Ti atomic ratio. The measured friction coefficients were found to be very similar for all the samples although a slight trend to decrease is observed. Conversely, more differences are noticed in the variation of the film wear rates as displayed in Fig. 7b. The best wear resistance is found for samples with the lowest Ag/Ti ratios (<6.3 at.% Ag). These coatings show typical values in the range of 5-8×10^{-6} mm^3/Nm whilst further Ag/Ti ratios led to a continuous degradation of the wear resistance. In order to obtain more information about the processes in the sliding contact, the surface of a ball scar from a sample with an intermediate Ag content was examined by SEM/EDX and Raman spectroscopy. Fig 8a shows the aspect of the alumina ball after have been tested against the Ag/Ti=0.40 film (10.8 at.% Ag). Material from the film and the solution can be detected adhered to the ball. The Raman spectrum obtained from three different points of the transferred material, displayed as P1, P2 and P3 in Fig. 8b, is dominated by the presence of the D and G bands at 1364 and 1583 cm^{-1} respectively, corresponding to the presence of aromatic six-membered sp^2 clusters and the sp^2 C-C bonds. A small peak at 235 cm^{-1} is attributed to TiC_yN_{1-y} as observed in previous papers of TiCN and TiAlCN coatings [31,32]. A chemical analysis was carried out by SEM/EDX after covering the ball by a thin Au layer in order to avoid the charge effects. The EDX spectrum (shown in Fig. 8c) revealed the presence of the elements forming the film (Ag, Ti, C, N) and Ca, probably from the FBS solution, besides of Au and Al, from the cover layer and the alumina ball respectively. In Fig. 9 it is depicted the Raman spectra taken from the wear track and compared with that obtained on the initial film. The spectra look like very similar showing both the D and G bands at 1364

and 1583 cm^{-1} respectively characteristic of a disordered carbon-based structure. The main differences are noticed if compared to the transfer film onto the ball, where the peaks were observed to be narrower and more separated in agreement with the behaviour observed in DLC and other amorphous carbon-based materials after friction modification [33]. Therefore, it can be concluded that the friction process takes place between this adhered layer, mainly formed by graphitic-like carbon, and the modified surface layer in the FBS liquid media. The almost constant value of the friction coefficient of 0.3 measured for the different Ag-TiCN coatings pointed to a similar nature of the counterfaces independently of the lubricant phase contents (Ag and CN_x). Lower friction coefficient values and higher-dependence with phase composition have been usually reported in silver-containing [5,34] and amorphous carbon-based phases [21,35] when tested in dry lubricant conditions. However, in presence of a liquid media (FBS in our case), the self-lubricant properties of these soft phases are less influencing [36]. Nevertheless, a beneficial effect in the topmost layers by the supply of self-lubricant silver and a-C phases should not be discarded. On the other hand, there are significant differences in terms of the wear resistance as a function of the Ag content that can be explained by the differences in the phase composition and the mechanical properties of the coating. As denoted in Fig. 6, the samples with higher contribution of hard TiC_yN_{1-y} phases, i.e. those with lower Ag content, are harder and thereby more resistant to the mechanical contact exhibiting lower wear rates.

3.4. Cytotoxicity

In order to verify the applicability of the coated samples as biomaterials, samples were assayed in terms their effect on fibroblasts cells (cytotoxicity). The cytotoxicity of the coatings was analyzed using the MTS assay with fibroblasts which gives the

indication of materials' toxicity on cells in a precise, fast and reliable way [37]. The cellular inhibition as a function of the Ag/Ti atomic ratio is shown in Fig 8. For Ag/Ti ratios < 1, there is an inhibition below 10% independently of the silver concentration. However, for the sample with the highest Ag content (Ag/Ti = 1.49) the toxicity is increased to about 20%. Several recent studies have already highlighted the toxicity of silver nanoparticles to various cultured cells [38, 39]. However, in the present studies, all samples show a mortality rate inferior to 20%, which is very acceptable, and especially in the range of low-medium Ag/Ti ratios, where a good compromise can be obtained between tribomechanical properties and biocompatibility. This would mean that Ag-TiCN coatings with low-medium Ag/Ti atomic ratio (Ag/Ti < 0.77) can now be tested concerning their antimicrobial properties.

4. Conclusions

Ag-TiCN thin films were deposited by reactive magnetron sputtering with variable silver content (0 to 26.7 at.%). The coatings were found to be a mixture of TiC_xN_{1-x}, Ag and a-$C(N)_x$ phases whose relative proportion varied depending on the Ag/Ti ratio. By means of XRD and XPS analysis it could be concluded that the proportion of soft phases becomes dominant and there was a substantial reduction in the grain size of TiC_xN_{1-x} for Ag/Ti>0.4, decreasing the hardness and the wear resistance. The friction coefficient was relatively constant (0.25-0.29) as it proceeds from sliding of a transferred material layer and the modified film surface in the FBS liquid media. The best hardness and wear resistant coatings were obtained for low Ag contents (up to 6.3 at. % of Ag or Ag/Ti < 0.20) with hardness of 18 GPa and specific wear rate values in the range of 10^{-6} mm^3/Nm. Moreover, the lower toxicity of samples with lower Ag/Ti content, was demonstrated by citotoxicity assays, displaying a death cell percentage

inferior to 10%. We conclude that incorporation of silver into protective carbon-based coatings for use in implant and medical devices must be limited up to 6 at.% to ensure a good balance between tribological and biomaterial properties.

Acknowledgments

The authors are grateful to the financial support of the CRUP Institution by the project "Acção Nº E – 1007/08", the Spanish Ministry of Science and Innovation (projects FUNCOAT CSD2008-00023 and HP2007-0116), Junta de Andalucía (project TEP 06782) and CSIC-FCT institutions (2007PT0043). The work was financially supported by Portuguese national funds through the FCT-Fundação para a Ciência e a Tecnologia, (project PTDC/CTM/102853/2008) and partially sponsored by FEDER funds through the program COMPETE - Programa Operacional Factores de Competitividade.

References

[1] A. U. Daniels, F. H. Barnes, S.J. Charlebois, R.A. Smith, J. Biomed. Mat. Res, 49 (2000) 469.

[2] S. Mandl, B. Rauschenbach, Surf. Coat. Technol. 156 (2002) 276.

[3] D. V. Shtansky, D. V. Levashov, N. B. Glushankova, N. B. D´yakonova et al. Surf. Coat. Technol. 182 (1) (2004) 101.

[4] R. Hauert, Diamond Relat. Mater. 12 (2003) 583.

[5] P.J. Kelly, H. Li, K.A. Whitehead, J. Verran, R.D. Arnell, I. Iordanova, Surf. Coat. Technol. 204 (2009) 1137.

[6] M.L. Morrison, R.A. Buchanan, P.K. Liaw, C.J. Berry, R.L. Brigmon, L. Riester, H. Abernathy, C. Jin, R.J. Narayan Diamond Relat. Mater. 15 (2006) 138-46.

[7] C.H. Kwok, W. Zhang, G.J. Wan, D.R. McKenzie, M.M.M. Bilek, P.K. Chu, Diamond Relat. Mater. 16 (2007) 1353.

[8] J.L. Endrino, A. Anders, J.M. Albella, J.A Horton, T.H. Horton, P.R. Ayyalasomayajula, M. Allen, Journal of Physics: Conference Series 252 (2010) 012012.

[9] N. Stobie, B. Duffy, D.E. McCormack, J. Colreavy, M. Hidalgo, P. McHale, S.J. Hinder, Biomaterials. 29 (2008) 963.

[10] D.P. Dowling, A.J. Betts, C. Pope, M.L. McConnel, R. Elloy, M.N. Arnaud, Surf. Coat. Technol. 163-164 (2003) 637.

[11] T. de los Arcos, P. Oelhafen, U. Aebi, A. Hefti, M. D.uggelin, D. Mathys, R. Guggenheim, Vacuum 67 (2002) 463.

[12] J.L. Endrino, J.J. Nainaparampil, J.E. Krzanowski, Surf. Coat. Technol. 157 (2002) 95.

[13] N.M. Chekan, N.M. Beliauski, V.V. Akulich, L.V. Pozdniak, E.K. Sergeeva, A. N. Chernov, V.V. Kazbanov, V.A. Kulchitsky, Diamond Relat. Mater. 18 (2009) 1006.

[14] P.J. Kelly, H. Li, P.S. Benson, K.A. Whitehead, J. Verran, R.D. Arnell, I. Iordanova, Surf. Coat. Technol. 205 (2010) 1606.

[15] P.J. Kelly, K.A. Whitehead, H. Li, J. Verran, R.D. Arnell, J. Nanosci. Nanotechnol. 11 (2011) 5383.

[16] C. Oliveira, L. Goncalves, B.G. Almeida, C.J. Tavares, S. Carvalho, F. Vaz, R.E. Galindo, M. Henriques, M. Susano, R. Oliveira, Surf. Coat. Technol. 203 (2008) 490.

[17] C. Oliveira, R.E. Galindo, C. Palacio, L.Vazquez, A. Espinosa, B.G. Almeida, M. Henriques, S. Calderon, S. Carvalho, Thin Solid Films 518 (2010) 5694.

[18] N. K. Manninen, R. Escobar Galindo, N. Benito, N.M. Figueiredo, A. Cavaleiro, S.Carvalho, "Ag-Ti(C,N)-based coatings for biomedical applications: influence of silver content on the structural properties", Journal of Physics D: Applied Physics 44 (2011) 375501.

[19] J.M. Antunes, A. Cavaleiro, L.F. Menezes, M.I. Simões, J.V. Fernandes, Surf. Coat. Technol. 149 (2002) 27.

[20] G. Stoney, Proc. Roy. Soc. London A 82 (1909) 172.

[21] D. Martínez-Martínez, C. López-Cartes, A. Fernández, J.C. Sánchez-López, Surf. Coat. Technol. 203 (2008) 756.

[22] D. Martínez-Martínez, C. López-Cartes, A. Justo, A. Fernández, J. C. Sánchez-López, Solid State Sciences 11(2009) 660.

[23] C.P. Mulligan, T.A. Blanchet, D. Gall,, Surf. Coat. Technol. 203 (2008) 584.

[24] S.J. Bull, D.G. Bhat, M.H. Staia, Surf. Coat. Technol. 163 –164 (2003) 499.

[25] A.P. Serro, C. Completo, R. Colaço, F. dos Santos, C. Lobato da Silva, J.M.S. Cabral, H. Araújo, E. Pires, B. Saramago, Surf. Coat. Technol. 203 (2009) 3701.

[26] E.J. Bienk, H. Reitz, N.J. Mikkelsen, Surf. Coat. Technol. 76 - 77 (1995) 475.

[27] J. Musil, Surf. Coat. Technol. 125 (2000) 322.

[28] J. Šůna, J. Musil, V. Ondok, J.G. Han, Surf. Coat. Technol. 200 (2006) 6293.

[29] J.L. Endrino, J.J. Nainaparampil, E. Krzanowki, Scripta Mater. 47 (2002) 613.

[30] E. Silva, M. Rebelo de Figueiredo, R. Franz, R. Escobar Galindo, C. Palacio, A. Espinosa, S. Calderon V. , C. Mitterer, S. Carvalho, Surf. Coat. Technol. 205 (2010) 2134.

[31] J.M. Lackner, W. Waldhauser, R. Ebner, R.J. Bakker, T. Schöberl, B. Major, Thin Solid Films 468 (2004) 125.

[32] C.P. Constable, J. Yarwood, W.-D. Münz, Surf. Coat. Technol. 116–119 (1999) 155–159.

[33] J.C. Sánchez-López, A. Fernández, in: A. Erdemir, C. Donnet (Eds.), Tribology of Diamond-Like Carbon Films: Fundamentals and Applications, Springer, New York, 2008, p. 311.

[34] K. Holmberg, A. Matthews, Coat. Tribology, Tribology series, 28 Ed. D. Dowson, Elsevier, 1994.

[35] J.C. Sánchez-López, D. Martínez-Martínez, M.D. Abad, A. Fernández, Surf. Coat. Technol. 204, 947-954 (2009).

[36] J. L. Endrino, J.C. Sánchez-López, R. Escobar Galindo, D. Horwat, A. Anders, Journal of Physics: Conference Series 252 (2010) 012005.

[37] G. Malich, B. Markovic, C. Winder, Toxicology 124 (1997) 179.

[38] P. V. AshaRani, G. L.K. Mun, M. P. Hande, S. Valiyaveettil, ACS Nano. 3 (2009) 279.

[39] K. Kawata, M. Osawa, S. Okabe, Environ. Sci. Technol. 43 (2009) 6046.

Figure Captions

Fig. 1. XRD patterns of the Ag-TiCN coatings deposited by DC reactive magnetron sputtering, with different Ag/Ti atomic ratios.

Fig. 2. C1s (a) and N 1s (b) photoelectron spectra for 4 representative coatings with Ag/Ti ratios of 0, 0.20, 0.40 and 1.49.

Fig. 3. Phase composition of the samples prepared with Ag/Ti ratios of 0, 0.20, 0.40 and 1.49.

Fig. 4. Cross-sectional SEM micrographs for samples with atomic ratios Ag/Ti: a) 0; b) 0.20; c) 0.40 and d) 1.49.

Fig. 5. Hardness and residual stress values of Ag-TiCN coatings vs. the Ag/Ti atomic ratio.

Fig. 6. Variation of the hardness and wear rate properties as a function of the ratio of soft (Ag+CN_x)/hard (TiC_yN_{1-y}) phases.

Fig. 7. Friction coefficient (a) and wear rate (b) values of Ag-TiCN as a function of the Ag/Ti atomic ratio.

Fig. 8. Optical micrograph of the alumina ball after the friction test onto the Ag-TiCN coating with 10.8 at. % of Ag (a) and corresponding Raman spectra (b) and EDX (c) analysis.

Fig. 9. Optical micrograph of the wear track after the friction test of the Ag-TiCN coating with 10.8 at. % of Ag (a) and corresponding Raman spectra (b).

Fig. 10. The rate of inhibition of cellular as a function of the Ag/Ti atomic ratio, after 7days incubation.

Table 1 R1

Table 1. Chemical composition and tribomechanical properties of the deposited Ag-TiCN coatings.

Sample	**Chemical composition** at. %				**Thickness** μm	**H** GPa	**σ** GPa	**μ**	**K** mm^3/Nm
Ag/Ti	Ag	Ti	C	N					
0	0	36.9	29.2	33.9	2.9	17.0	-0.5	0.29	7.1E-06
0.06	2.0	35.1	29.9	33.0	2.0	17.8	-1.0	0.31	1.9E-05
0.15	4.6	31.1	32.4	31.9	2.4	18.2	-1.4	0.25	5.3E-06
0.20	6.3	31.6	30.5	31.6	1.4	18.0	-1.7	0.26	5.2E-06
0.27	8.0	29.2	29.5	33.3	1.5	16.5	-1.8	0.27	2.8E-05
0.40	10.8	26.9	31.2	31.1	3.0	15.0	-2.5	0.27	3.8E-05
0.77	19.8	25.7	30.6	23.9	2.9	10.0	-1.6	0.28	4.8E-05
1.49	26.7	17.9	33.6	21.8	3.2	8.0	-1.3	0.25	8.7E-05

Figure 1

Click here to download high resolution image

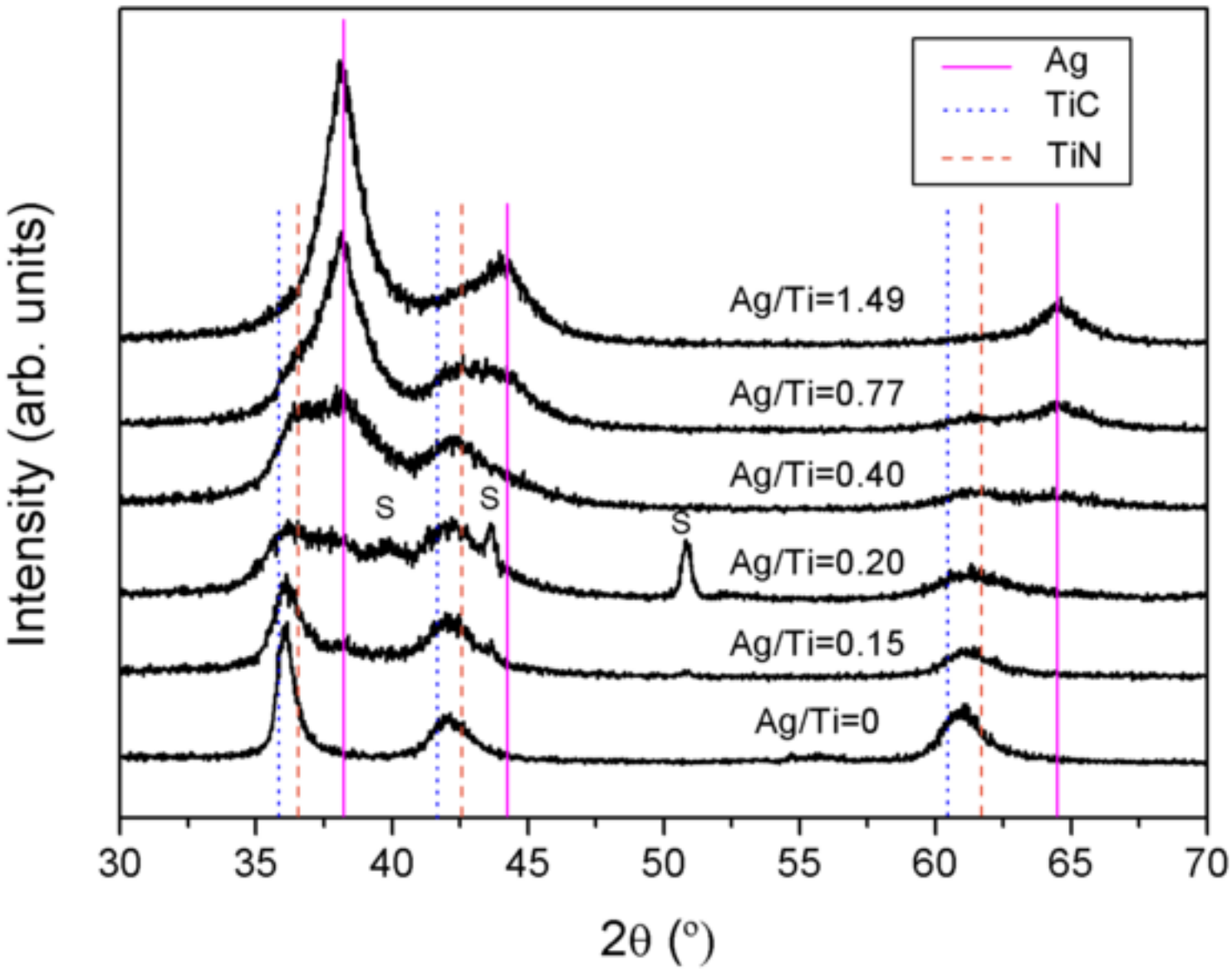

Figure 2a

Click here to download high resolution image

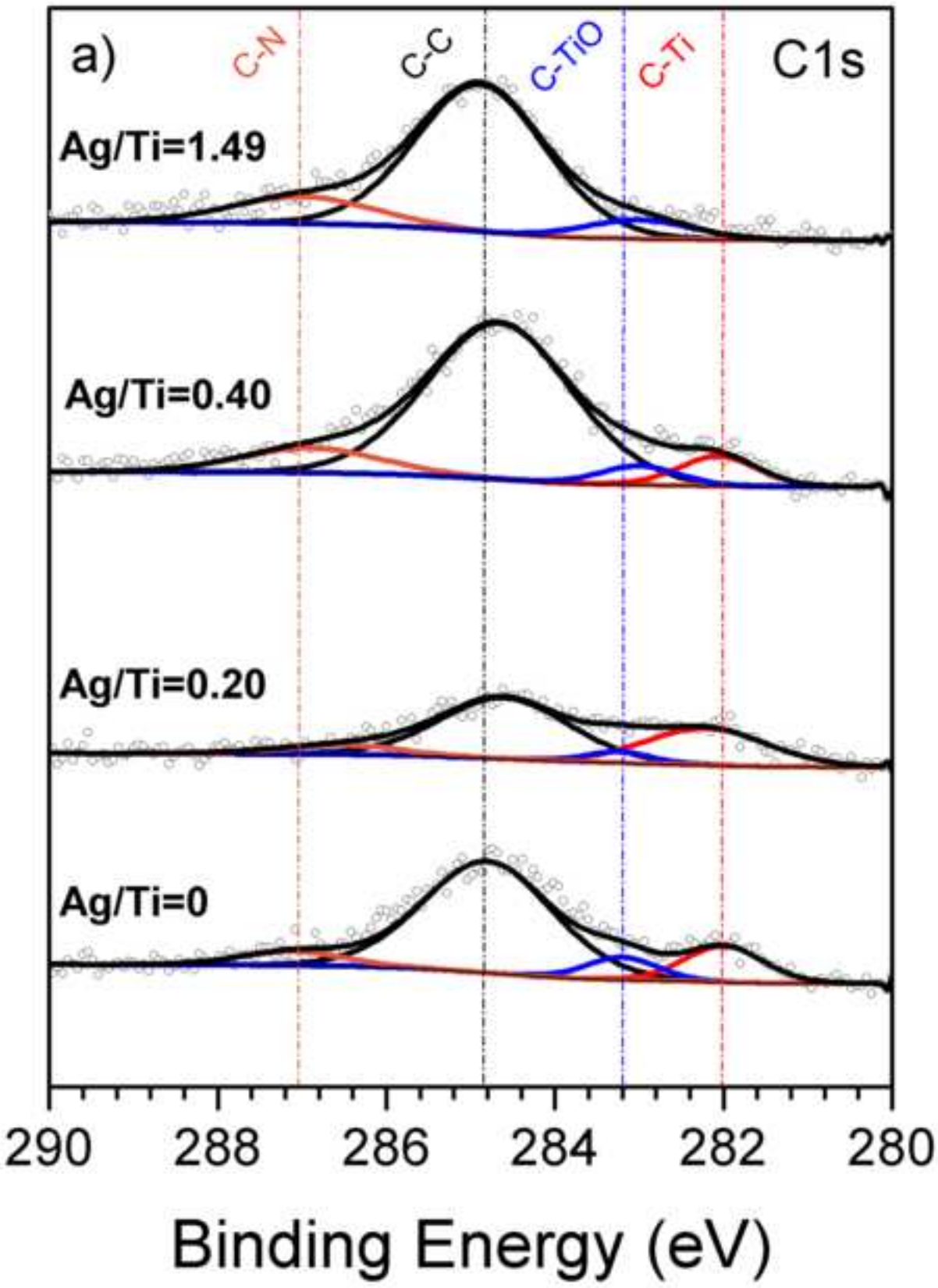

Figure 2b

Click here to download high resolution image

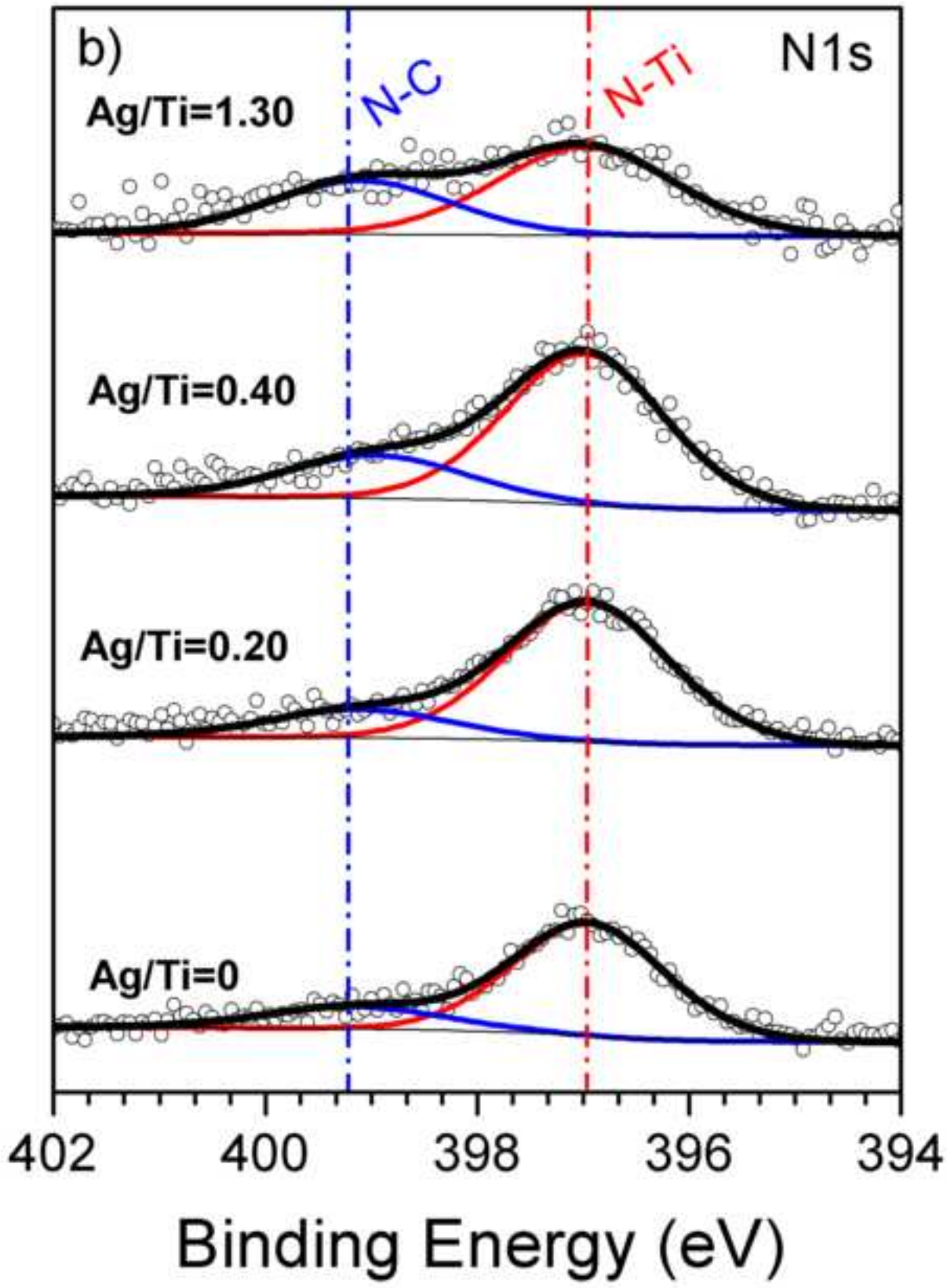

Figure 3
Click here to download high resolution image

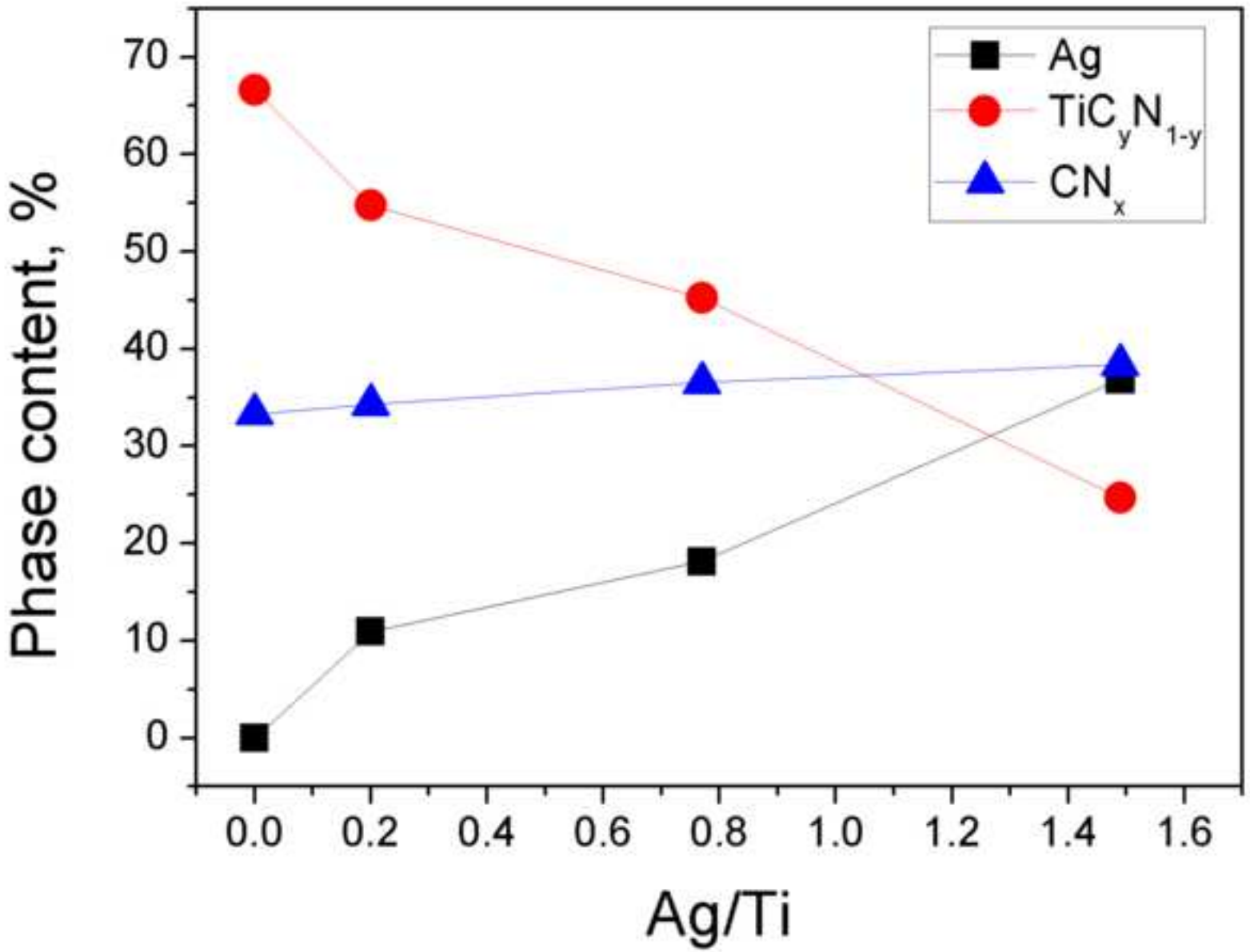

Figure 4

Click here to download high resolution image

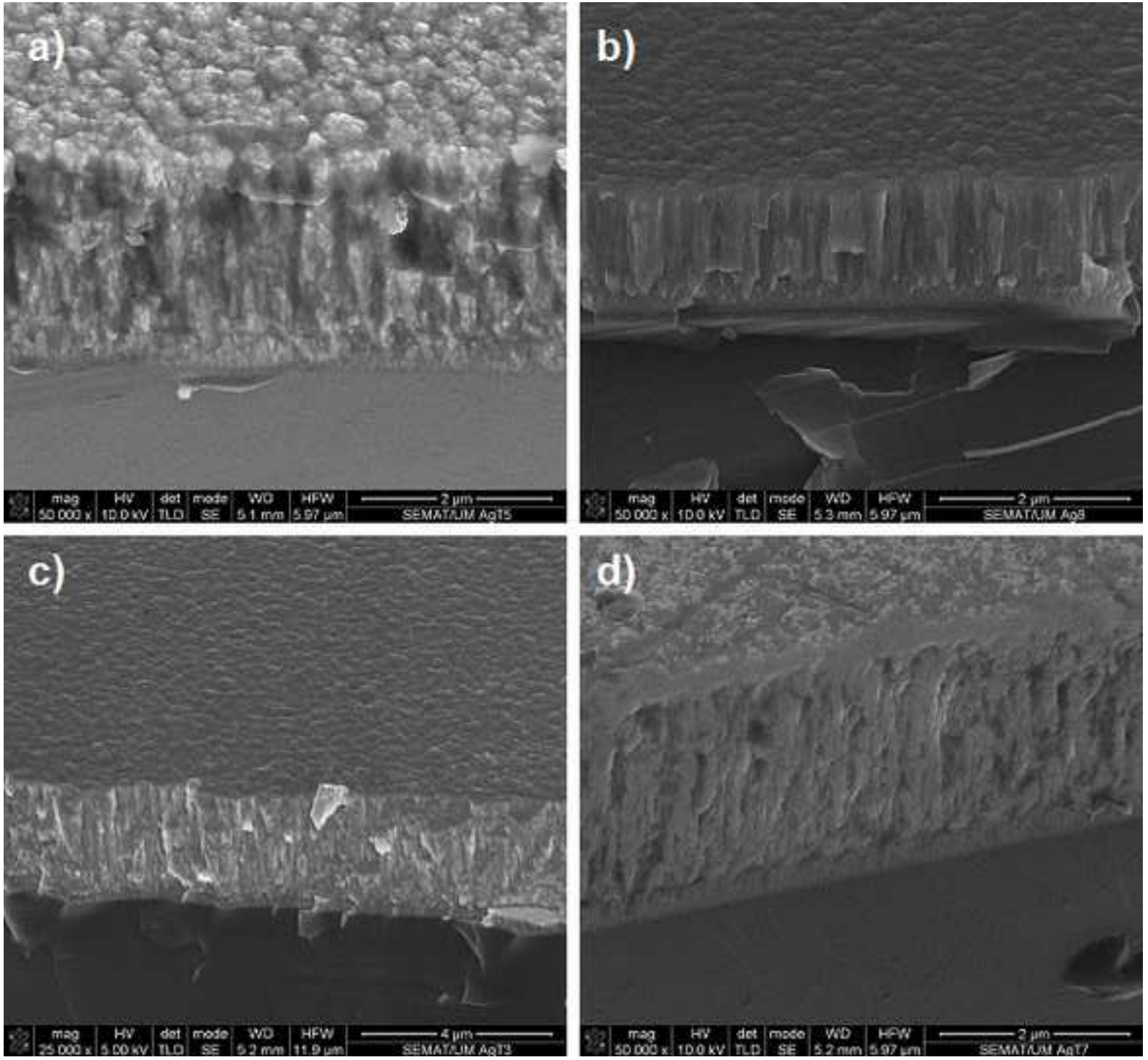

Figure 5

Click here to download high resolution image

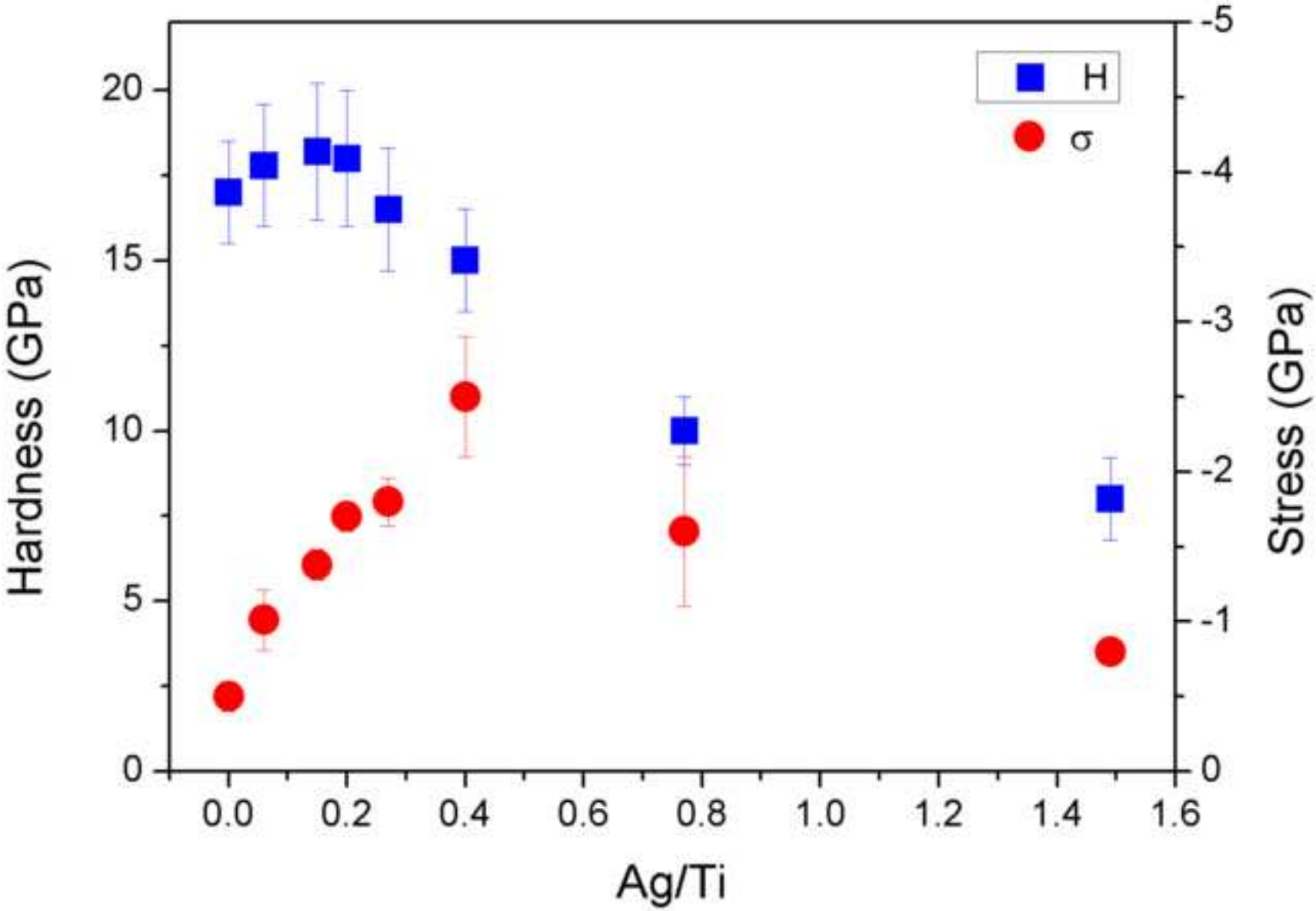

Figure 6

Click here to download high resolution image

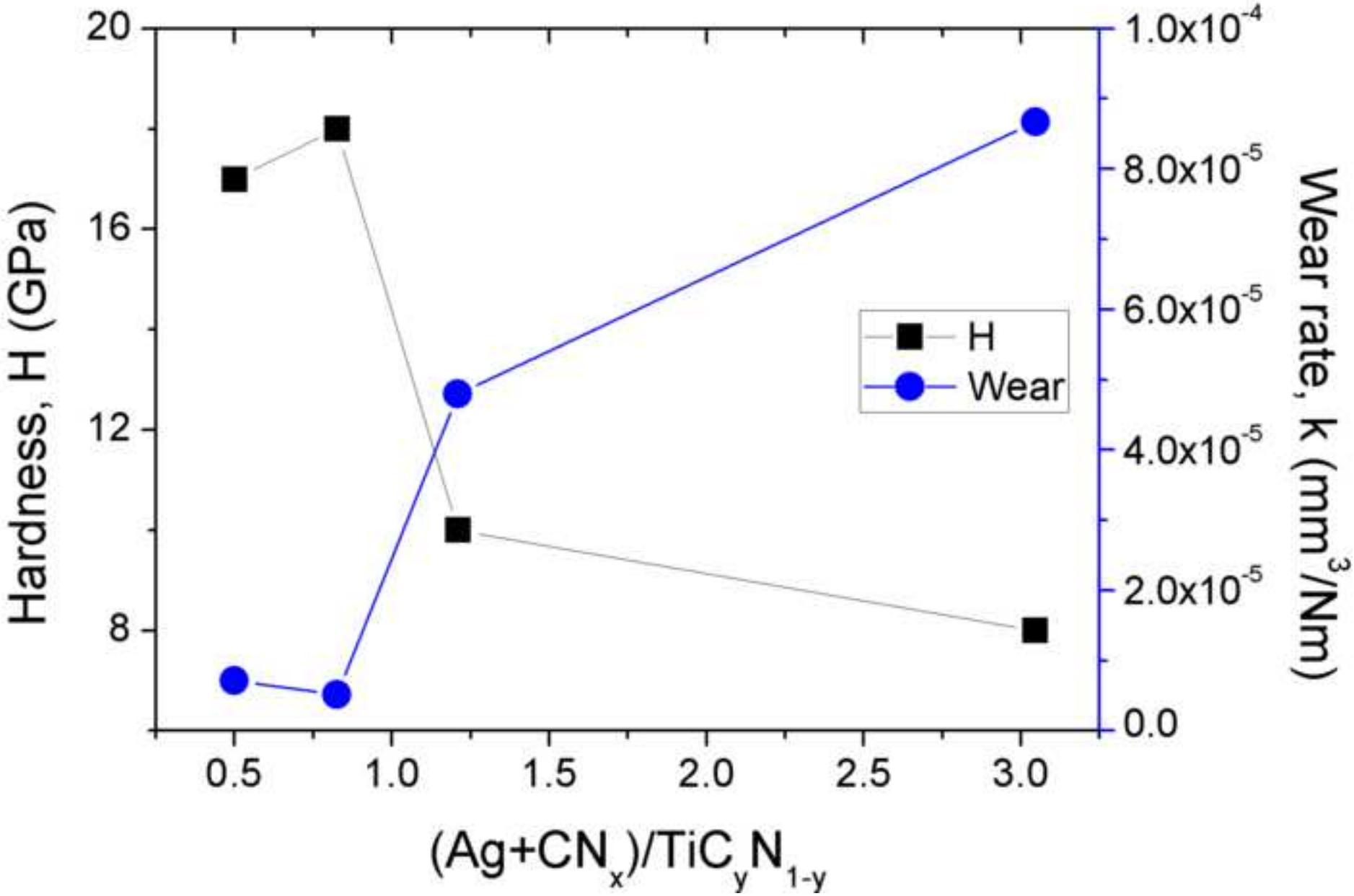

Figure 7
Click here to download high resolution image

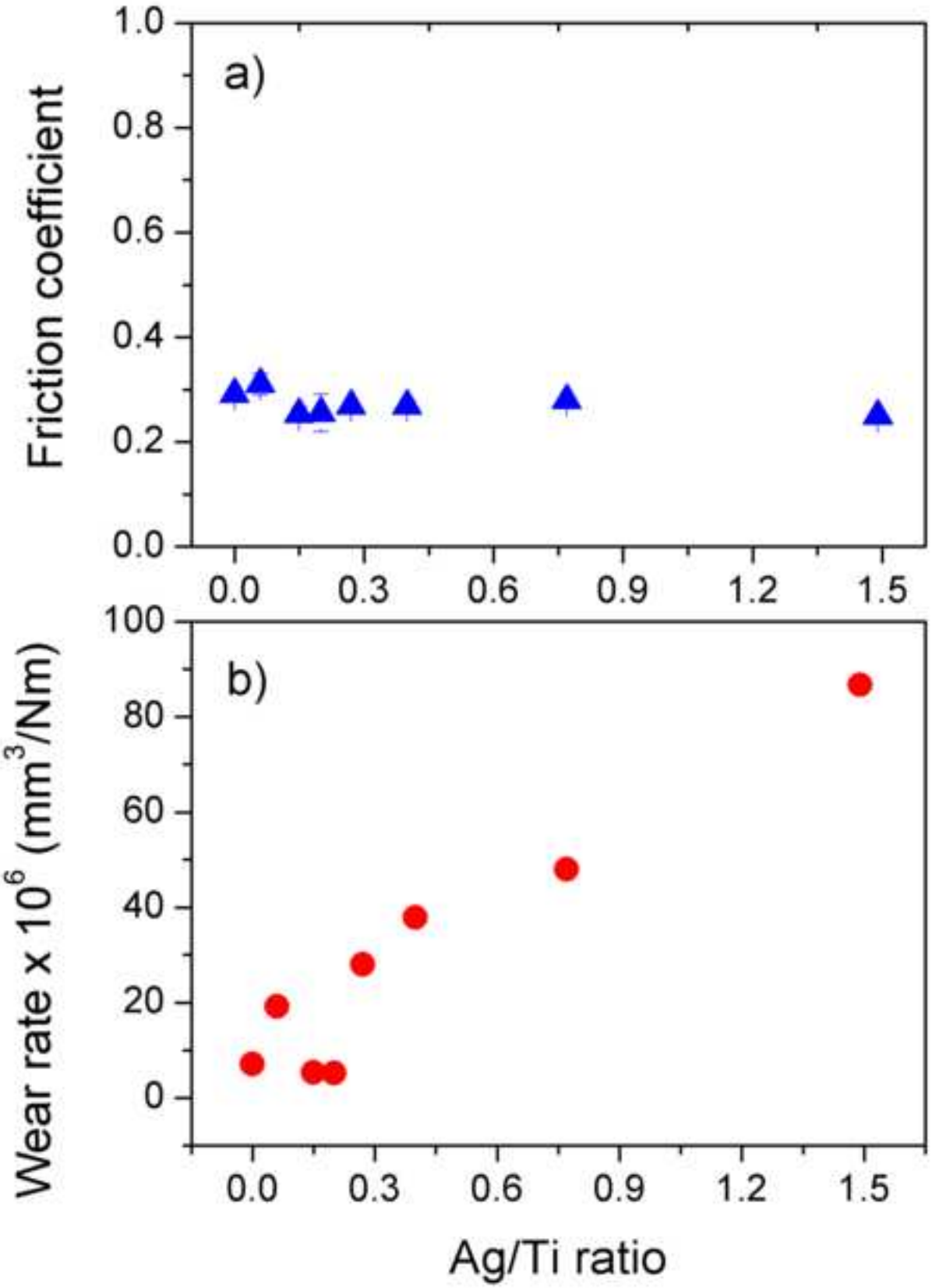

Figure 8

Click here to download high resolution image

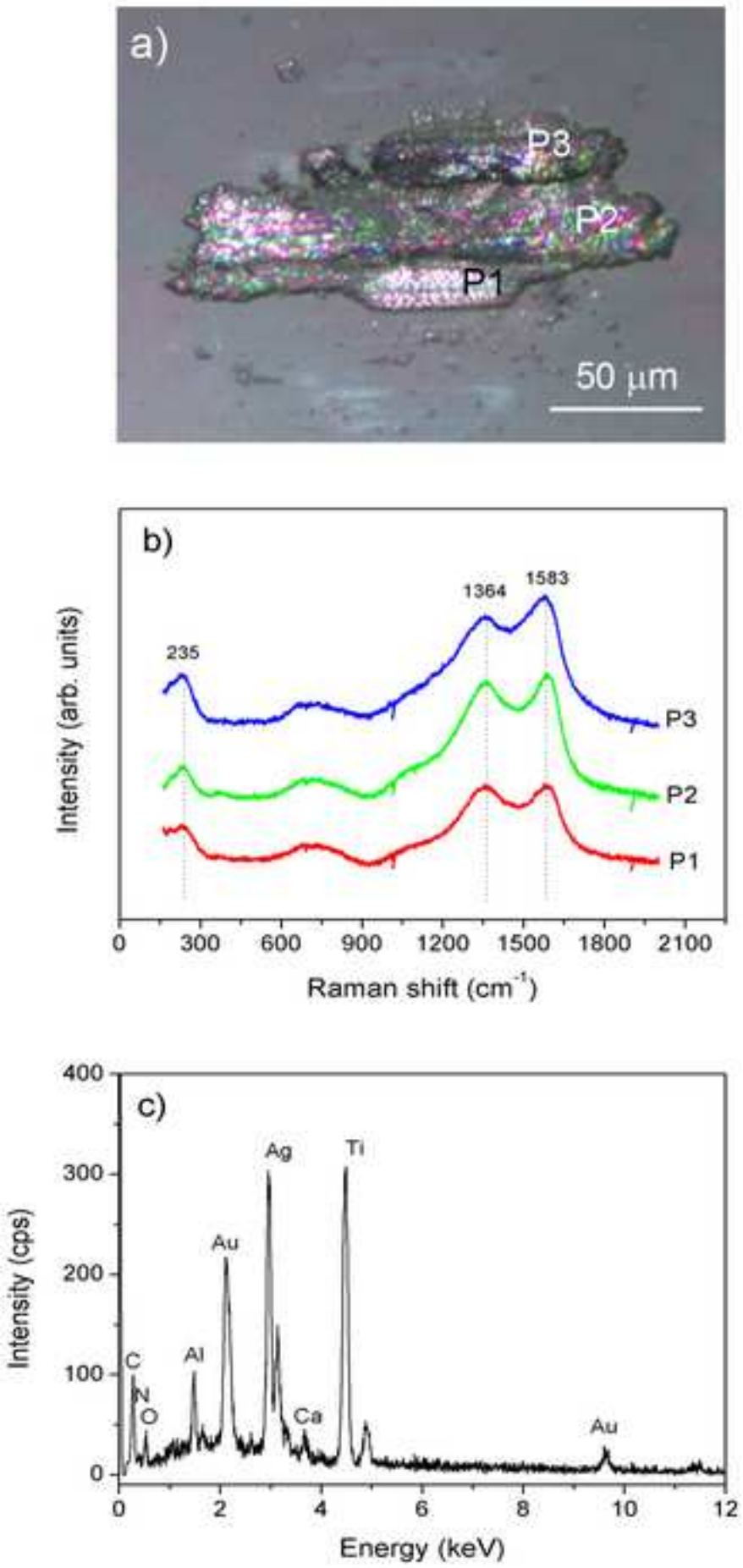

Figure 9
Click here to download high resolution image

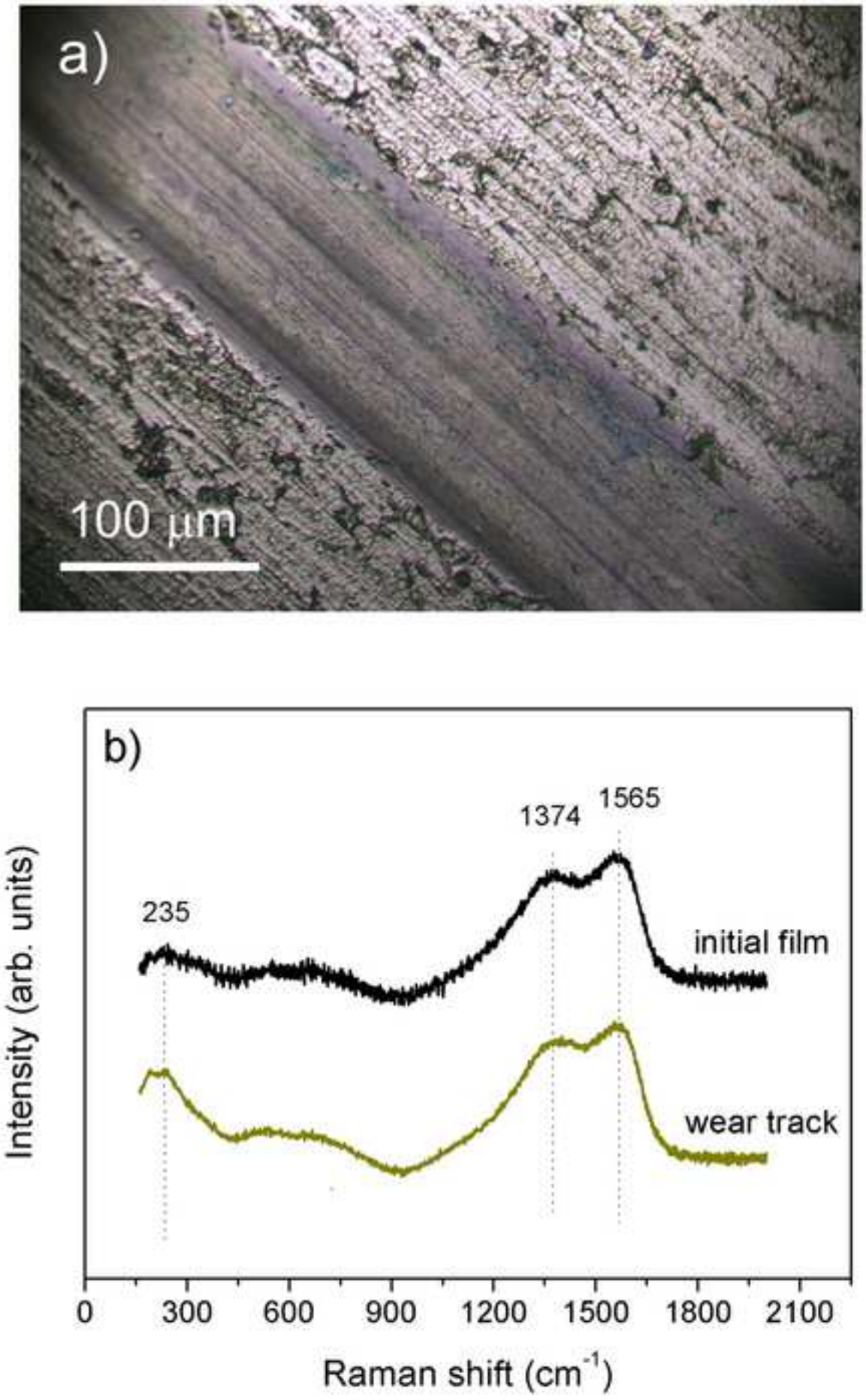

Figure 10
Click here to download high resolution image